ECRF Experiments for Local Heating and Current Drive in JT-60U

Y.IKEDA, S.IDE, T.SUZUKI, A.KASUGAI, K.TAKAHASHI, K.KAJIWARA, A.ISAYAMA, T.OIKAWA, K.HAMAMATSU, Y.KAMADA, T.FUJITA, K.SAKAMOTO, S.MORIYAMA, M.SEKI, R.YOSHINO, T.IMAI, K.USHIGUSA, T.FUJII, and the JT-60 TEAM
Japan Atomic Energy Research Institute, Naka Fusion Research Establishment
Naka-machi, Naka-gun, Ibaraki-ken 311-0193, Japan
E-mail:ikeda@naka.jaeri.go.jp

Abstract. An ECRF program has been started to study the local heating and current drive in JT-60U. The frequency of 110GHz was adopted to couple the fundamental O-mode from low field side with an oblique toroidal injection angle for current drive. Experiments were performed at the injection power of ~1.5 MW by using three gyrotrons, each of which has generated the output power up to ~0.8 MW for 3 seconds. A strongly peaked T_e profile was observed and the central electron temperature increased up to ~15 keV when the O-mode was absorbed on axis. The local electron heating clarified the significant difference on the heat pulse propagation between in the plasmas with the internal transport barrier (ITB) and without ITB. The driven current estimated by the Motional Stark Effect (MSE) diagnostic showed that the EC driven current was ~0.2MA at the local electron temperature and density of T_e ~6 keV, n_e~$0.7x10^{19}$ m^{-3}. The measured driven current near the axis was consistent with the theoretical prediction using a Fokker Planck code. In the case of co-ECCD, the sawteeth activity in NB heated plasma was completely suppressed for 1.5 s with the deposition at the inversion radius, while the sawteeth was enhanced for counter-ECCD at the same deposition condition.

1. Introduction

The EC heating is an appropriate method to investigate the characteristics of the reactor-equivalent plasma where the electron heating by α particle is dominant. The EC current drive, which can drive the plasma current in a small region, is an excellent actuator for control of the current profile. These properties of EC heating and current drive can be used to improve the plasma performance. Recently, significant progress has been achieved in the development of high-power, long-pulse gyrotron at the frequency of over 100GHz [1]. Then, the JT-60U has employed an 110 GHz ECRF system to inject the fundamental O-mode from low field side, which is the proposed scheme for ECCD in ITER. The ECRF system is composed of three RF units. Each unit has a gyrotron, which is designed to generate 1MW for 5 seconds by using a diamond window, and a transmission line of ~60 m in length and about 70% of the output power from the gyrotrons are injected into the plasma. The deposition position of EC wave is controlled during a plasma discharge by a poloidal steerable mirror with a toroidal injection angle of ~20˚. The wave refractive index parallel to the magnetic field ($N_{//}$) for the O-mode is designed about 0.5 at the plasma center. The measured Full Width Half Maximum (FWHM) of EC beam is 0.1 m at the center of vacuum vessel. The first unit started an operation in 1999 [2] and the conditioning of the each gyrotron has been done up to ~0.8 MW x 3 s. This paper reports the results of the local electron heating and current drive experiments in JT-60U at the total injection power up to ~1.5 MW with three units.

2. Absorption of the fundamental O/ X-mode for oblique injection

When the EC wave with perpendicular wave number is launched from low field side, the fundamental X-mode is not accessible to the resonance layer $\omega=\omega_{ce}$ due to the reflection at the cut-off density. However, the strong absorption of the fundamental X-mode occurs in the case of the oblique injection into a relatively low density, high temperature plasma due to the large Doppler effect of $\omega=\omega_{ce}/\gamma+k_{//}\bullet v_{//}$, where γ is the relativistic factor, $v_{//}$ is the parallel electron velocity, $k_{//}$ is the parallel wave number given by $k_{//}=\omega/c\bullet N_{//}$, and c is the light speed. Figure 1(a) and (b) show the typical time evolution of the central electron temperature at the

averaged density of 1.8 x10^{19}m^{-3} and 0.5 x10^{19}m^{-3}, respectively. The plasma current is 1.4 MA. The EC injections are performed in turn using three units at the power level of 0.5~0.6 MW. The EC beams from the steerable mirror are set toward the magnetic axis for all units. The power fraction of the O-mode of each unit is controllable by the polarizers in the transmission line. In this discharge, the power fractions of the O-mode component are estimated 85%, 35% and 35% for unit #1,#2 and #3, respectively, according to the measured wave polarizations in a low power test. The central electron temperatures increase (ΔT_{e0}) from 1.9 keV to 2.7 keV for unit #1 and from 2.0 keV to 2.3 keV for #2, #3 units, respectively, for the high density operation (E36679). It is found that the plasma response in ΔT_{e0} is in proportion to the power fraction of the O-mode component at the high density operation, while there is no difference in ΔT_{e0} between unit #1 and unit #2, #3 at the low density operation (E36656). This result indicates that the fundamental X-mode is directly absorbed at the low density operation. Indeed, the ray-tracing code shows that the absorption of the fundamental X-mode occurs as shown in Fig. 2. In this calculation, the central electron temperatures for E36656 and E36679 are given 8 keV, 2.3 keV, respectively. The wave rays of the O-mode for both density cases are not diffracted and their powers are almost absorbed near the plasma center. The X-mode is reflected near the plasma surface in high density case, while the X-mode is more locally absorbed near the plasma center than the O-mode at the low density case. The critical density limit of the X-mode absorption is about $\bar{n}_e$~0.6x10^{19} m^{-3} for T_{e0}~8keV in the ray tracing analysis.

By checking the plasma response in T_e at high density operation, the power fractions of O-mode component have been adjusted at 80~90% for all units by using the polarizers. Thus, the total absorption power are about 80-90% of the injected power except the low density condition less than $\bar{n}_e$~0.6x10^{19} m^{-3}.

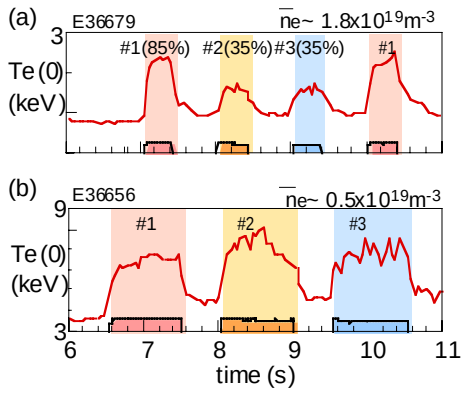

Fig.1 Multi-pulse injections of different power fraction of O-mode component ; (#1:85%, #2:35%, #3:35%). (a) $\bar{n}_e$~1.8x10^{19}m^{-3}, (b) $\bar{n}_e$~0.5x10^{19} m^{-3}.

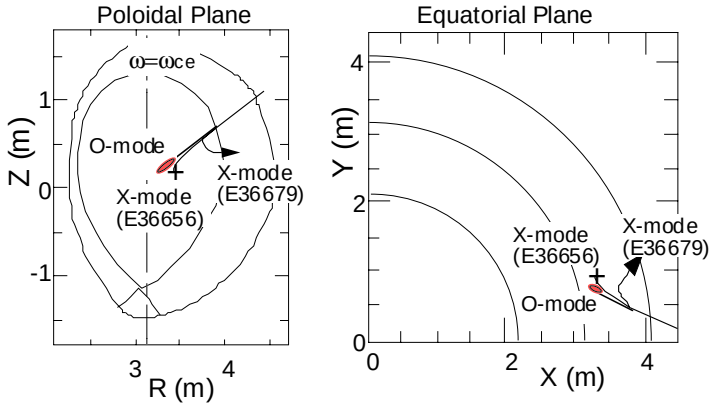

Fig.2 Ray trace of EC waves. The X-mode at low density discharge (E36656) is fully absorbed near the center (+), while the X-mode is reflected at high density discharge (E36679). The O-modes are almost absorbed at the hatching area along the ray for both cases.

3. Local electron heating

The strongly peaked T_e profile was obtained by keeping the EC deposition on axis as shown in Fig.3. The EC wave is injected just after plasma current build-up to avoid the sawteeth activity. The plasma current, the averaged electron density and the injected power are 1.4 MA, ~ 1x10^{19} m^{-3} and 1.5MW, respectively. Since the X-mode can not be absorbed in this density region, the absorbed power is ~1.3MW. The T_e profile was measured by the Ruby and YAG Thomson scattering diagnostics. The central electron temperature within r/a ~0.3 quickly increases less than 200~300 ms and the maximum T_{e0} reached up to more than 15 keV.

The loop voltage is reduced from 1.0 V to 0.5~0.6 V. The diamagnetic store energy is ~0.55 MJ and the total energy confinement time is 0.28 s. The typical electron thermal diffusivity (χ_e) evaluated from the power balance are less than 1 m^2/s inside the hot region and 2~3 m^2/s outside the hot region in this discharge. In the density range of 0.6~1.2x10^{19} m^{-3}, the data set of electron thermal energy contents, including the strongly peaked T_e plasma discharges, are in the range of the Rebut-Lallia scaling [3] and/or the half of the ITER89L-mode scaling. The contribution of the hot region to the global confinement seems to be small due to the small volume of the hot region.

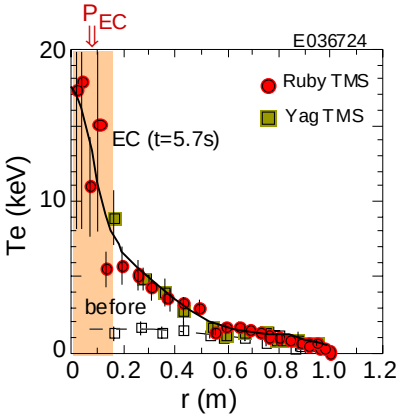

Fig. 3 Peaked T_e profile produced by EC alone

The investigation of the effect of electron heating to the confinement with the internal transport barrier (ITB) is a critical issue for the steady state fusion reactor with a high confinement and a high bootstrap current fraction. Figure 4 shows typical electron temperature profiles at 1s after EC injection in reversed magnetic shear (R/S) plasma with ITB. The plasma current is 1MA. The NB power of 5~10 MW is injected to form the R/S configuration with ITB during I_p ramp-up for delaying the current penetration, and is kept at ~5 MW during EC injection. The average and central densities are $\bar{n}_e$~1.2x10^{19} m^{-3} and n_{e0}~2.5-3x10^{19} m^{-3}, respectively. The EC power deposition is set on axis at the power of ~0.7MW. It is clearly found that the central electron temperature increases from 4 keV to 5.5 keV with keeping the flat T_e profile in the case of EC heating inside the ITB. There is no degradation of ion temperature with keeping the flat T_i profile (T_{i0} changed from ~6.5 to ~7.5 keV).

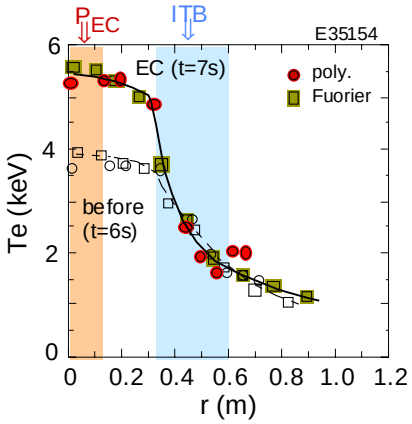

Fig. 4 Flat T_e Profile during EC heating inside ITB

The EC heating inside the ITB clearly shows the different properties of the thermal transport with (E35154) and without the ITB (E36849). Figure 5 shows the comparison of the contour plots of the increase of electron temperature ΔT_e measured by ECE diagnostics just after EC injection on axis. In the reference shot (E36849), the EC power of ~1.1 MW is injected into a positive magnetic shear plasma without ITB. The NB power and the averaged density are ~ 4MW, ~1.4x10^{19} m^{-3} in the reference shot. In the case of without ITB, the local power deposition is clearly observed in the ΔT_e within ~0.2 m from the axis and the ΔT_e is quickly saturated within 200ms, while there is no peaking in the ΔT_e near the deposition

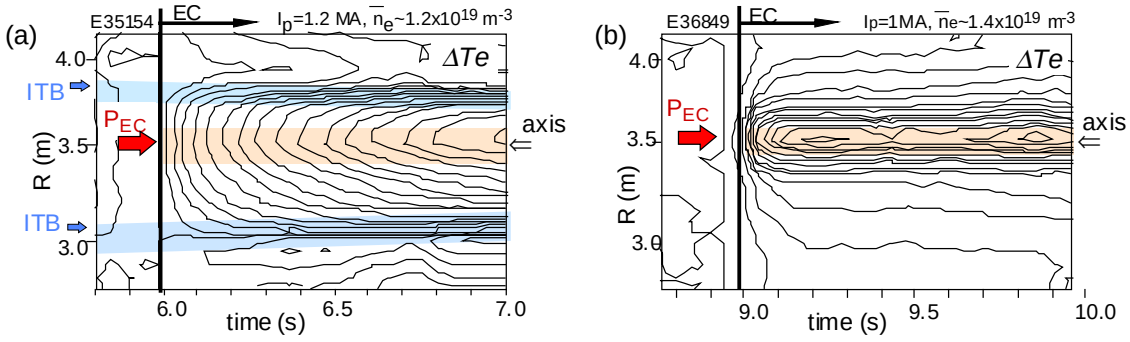

Fig. 5 Comparison of contours of ΔT_e with ITB (a) and without ITB (b). The EC waves are absorbed on axis in both cases. The ΔT_e between the contour lines is 0.1 keV.

position (the axis) and the whole electron temperature inside the ITB gradually increases in the case of with ITB. This indicates that the thermal transport inside the ITB is large, while it is reduced at the ITB. Detailed analysis of the electron thermal transport will be done by using EC power modulation in further work.

4. Control of local current profile

The current profile controllability of ECCD was studied by using a motional Stark effect (MSE) diagnostic in JT-60U. The current profile is evaluated by solving the Grad-Shafranov equation with the MSE pitch angle. Figure 6 (a) and (b) show the current density evaluated by the MSE pitch angle in the case of EC deposition at r/a~0.15 (near-axis:E36884) and r/a~0.25 (off-axis:E36807) by controlling the steerable mirror. The injected EC powers are about 1.3 MW (E36884) and 1MW (E36807) with co- direction at the plasma current of 1MA. In the near-axis case, the averaged and local densities at r/a~0.15 are ~0.5×10^{19} m^{-3} and ~0.7×10^{19} m^{-3}, respectively. The electron temperature at r/a~0.15 is 6 keV in ECCD. In the off-axis case, the averaged density is ~0.4×10^{19} m^{-3}. The local density and electron temperature at r/a~0.25 are ~0.5×10^{19} m^{-3} and 6 keV, respectively. The location of the change of the current density is consistent with the EC deposition position. It is confirmed that the local current profile is well controlled by steering the EC beam from the antenna.

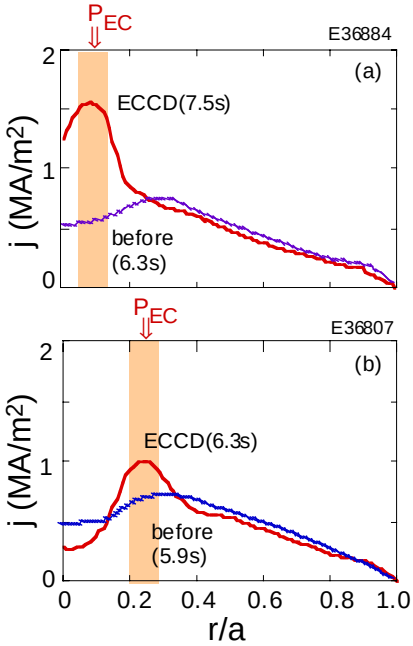

Fig.6 Current profile before and during ECCD estimated by MSE diagnostic, (a) EC deposition at r/a~0.15, (b) r/a~0.25

The local EC driven current can be estimated by subtracting the OH driven current, bootstrap current from the total current, where the OH driven current is given by the local electric filed. The profile of electric filed is evaluated by the reduction in loop voltage, which is estimated by the change of MSE pitch angle [4]. The bootstrap current is calculated by the transport analysis code. The NB for the MSE diagnostic is injected in balance to cancel the NB driven current in this experiment. In the analysis for the near-axis case, the local current density of ~2 MA/m^2 is observed near r/a=0.1 as shown in Fig 7. The uncertainties in the driven current are mainly due to the estimation of the local electric field. The total current integrated over the deposition area is 205±115 kA. The dotted line shows the theoretical calculation by using a quasilinear Fokker-Planck code [5], where the contribution of X-mode component is taken into account. The theoretical driven current is 243 kA. It is noted that the measured current density and driven current are almost consistent with the theoretical predictions in the near-axis case. In the analysis of the off-axis case, the uncertainties in the OH driven current is the same level of the measured total current at present. A detailed study with increasing the MSE channels is in progress.

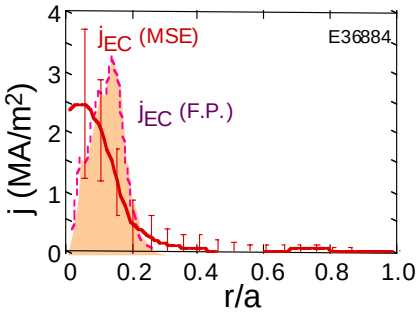

Fig. 7 EC driven current in the case of near-axis iniection

The effect of local ECCD was investigated on the suppression of sawteeth activity in the NB heated plasmas. Figure 8 shows the comparison of the sawteeth activities with co-ECCD (a) and counter-ECCD (b) at the plasma current of 1MA, where the EC deposition is set on the inversion radius. Since the toroidal injection angle of the antenna is fixed at ~20°, the counter-ECCD is performed by changing the direction of plasma current and toroidal

magnetic field. The NB power of 1.7 MW is injected in balance to cancel the NB driven current. The averaged densities are $1.2\times10^{19}m^{-3}$ for co-ECCD and $1.0\times10^{19}m^{-3}$ for counter-ECCD. The locations of the inversion radius before EC injection are at r/a~0.15 for both cases. The EC power of 1.2 MW is injected to be absorbed at r/a~0.15. The expected absorbed power, power density and EC driven current density at the inversion radius are ~1MW, ~0.4 MW/m^3 and ~0.4 MA/m^2 respectively. It is found that completed sawteeth suppression is obtained in the case of co-ECCD. The sawteeth period before EC injection is 300ms, and the sawteeth is fully suppressed during EC injection. After EC injection, the sawteeth appears again and its period becomes short at 200ms probably due to the penetration of plasma current. In the case of counter-ECCD with the absorption at the inversion radius, the sawteeth activity is enhanced as shown in Fig.8(b). It is noted that the sawteeth period during EC injection becomes shorter than that of NB heated plasma. The sawteeth periods are 150 ms, 250ms at the EC power of ~1MW, ~0.6 MW, respectively. The electron temperatures near the inversion radius are ~5keV for both cases, so the change of the local resistance is not major reason to explain the effect of sawteeth suppression. This result suggests that the mechanism of the sawteeth suppression is the change of q profile as reports of the sawteeth control by ECCD in OH plasmas [6,7]. Together with analyzing the current profile in detail, further study is required to clearly explain the mechanism of sawteeth suppression.

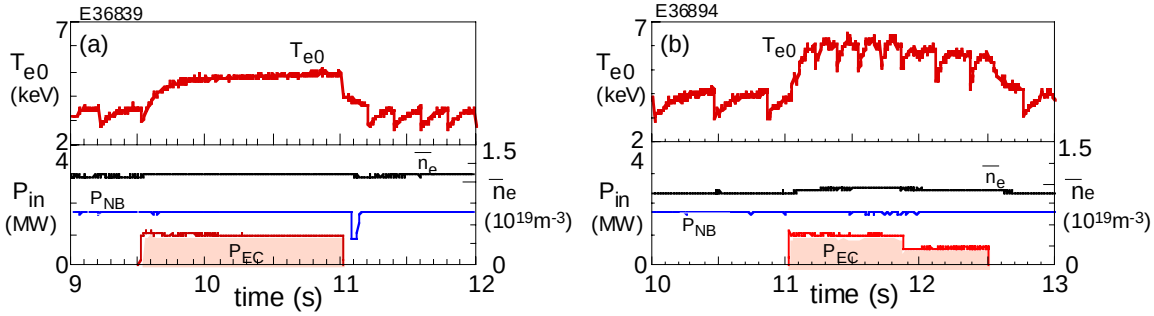

Fig. 8 Comparison of sawteeth activities with co-ECCD (a), and counter-ECCD (b) at the inversion radius.

Reference

[1] K. SAKAMOTO et al., "High power 170 GHz gyrotron with synthetic diamond window", Review of Scientific Instruments **70** (1999) 208.

[2] Y. IKEDA et al., "Initial Results of ECRF Operation and Experiments in JT-60U", Fusion Eng. And Design (in press).

[3] P.H. REBUT et al., "The critical temperature gradient model of plasma transport: applications to JET and future tokamaks", Plasma Physics and Controlled Nuclear Fusion Research 1988, (Proc. 12th Int. Conf. Nice, 1988), IAEA, Vienna (1989).

[4] T.C. LUCE et al., "Current profile modification with electron cyclotron current drive in the DIII-D tokamak", Fusion Energy 1998 (Proc. 17th Int. Conf. Yokohama, 1998), IAEA, Vienna (1999).

[5] K. HAMAMATSU, "Numerical study for positional control of ECCD by the Ordinary wave in a tokamak plasma", J. of Plasma and Fusion Research **75** (1999) 143.

[6] D.A. KISLOV et al., "ECCD and ECH effect on sawtooth oscillations in T-10", Controlled Fusion and Plasma Physics (Proc. 22nd Eur. Conf. Bournemouth, 1995), Vol. 19C, Part I, European Physical Society, Geneva (1995) 369.

[7] M. ASAKAWA et al., "Sawtooth control by on-axis electron cyclotron current drive on the WT-3", Fusion Energy 1998 (Proc. 17th Int. Conf. Yokohama, 1998), IAEA, Vienna (1999).